N/P co-doping regulates the local microcrystalline structure of hard carbon to facilitate sodium-ion storage

Yujie Guo [a, 1], Ke Liu [a, 1], Jie Xiao [a], Xiaoyuan Zeng [a, *], Shun Ji [a], Yanjia Zhang [a], Peng Dong [a, *], Ziyi Zhu [a, *]

[a] *National and Local Joint Engineering Research Center for Lithium-ion Batteries and Materials Preparation Technology, Key Laboratory of Advanced Battery Materials of Yunnan Province, Faculty of Metallurgical and Energy Engineering, Kunming University of Science and Technology, Kunming 650093, China.*

Corresponding authors

**E-mail*: zengxiaoyuan@kust.edu.cn (X. Zheng); dongpeng2001@126.com (P. Dong); zyzhu23@kust.edu.cn (Z. Zhu).

1 Figures

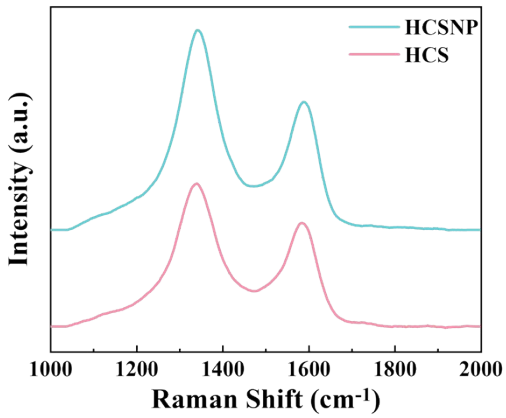

Fig. S1. Raman spectra of HCS and HCSNP.

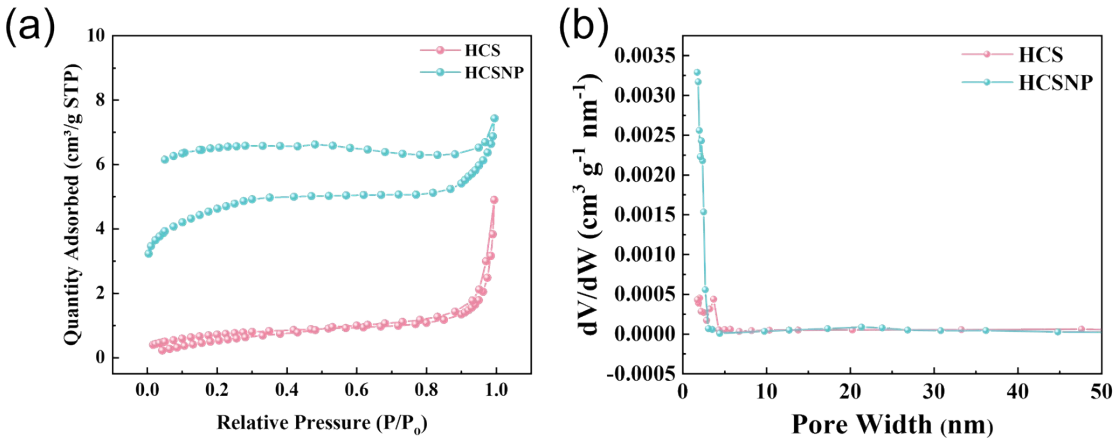

Fig. S2. (a) N_2 adsorption-desorption isotherms and (b) Pore width distributions of HCS and HCSNP.

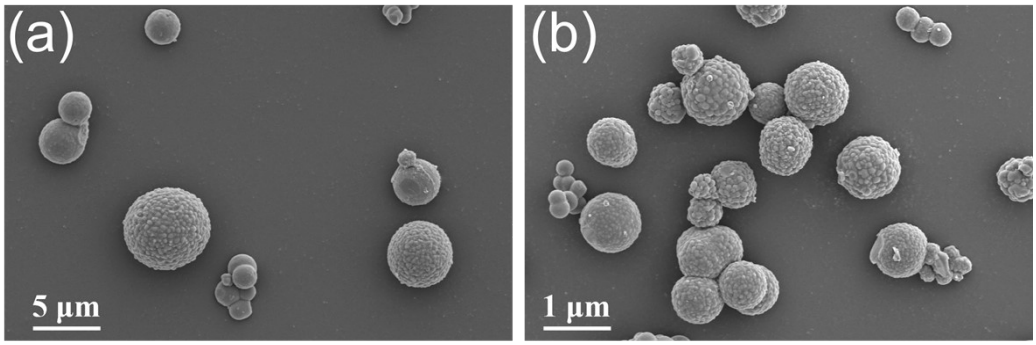

Fig. S3. SEM images of (a) HCS and (b) HCSNP.

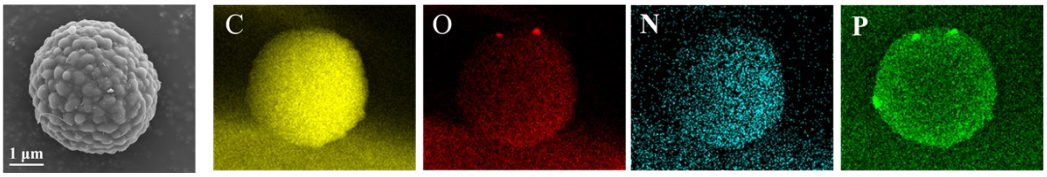

Fig. S4. SEM image and EDS energy spectrum of HCS.

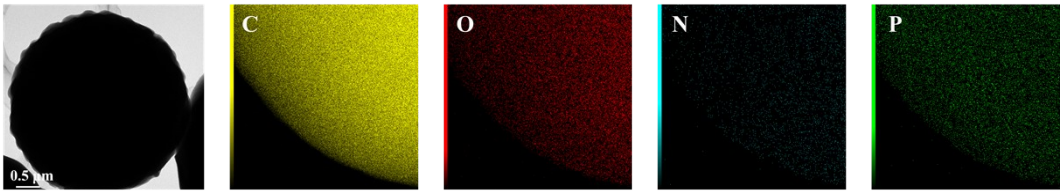

Fig. S5. TEM images of HCSNP and the corresponding Mapping elemental analysis.

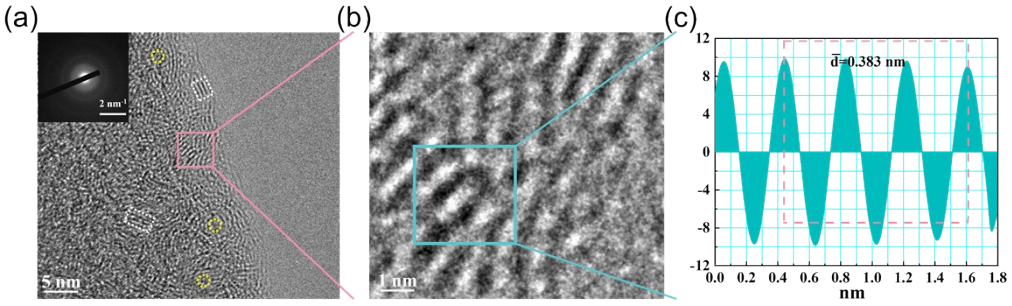

Fig. S6. (a, b) HRTEM images and the corresponding SAED images of HCS; (c) The lattice spacing after Fourier transformation.

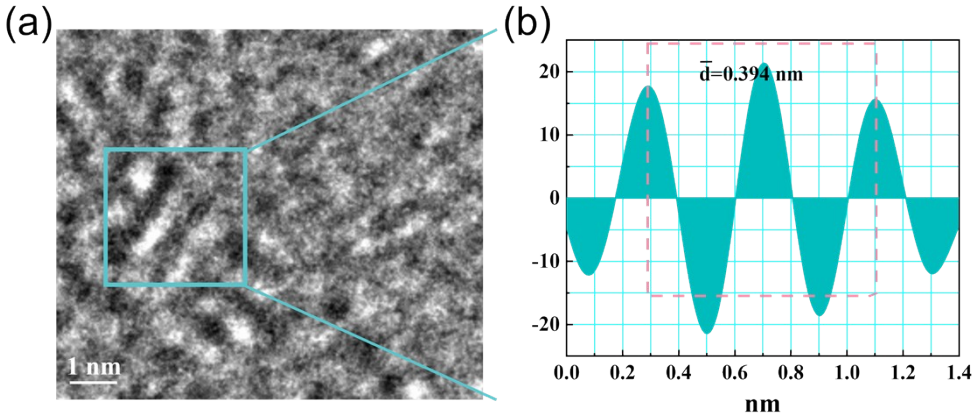

Fig. S7. (a) HRTEM images of HCSNP; (c) The lattice spacing after Fourier transformation.

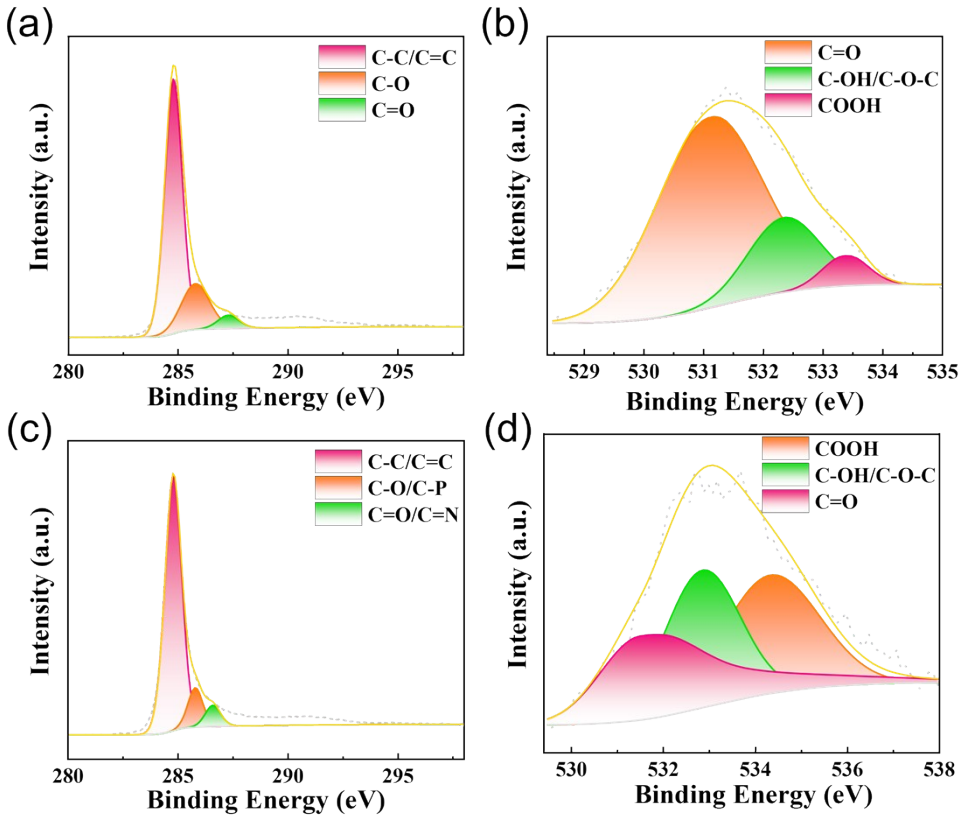

Fig. S8. High resolution energy spectra of C 1s and O 1s of (a, b) HCS and (c, d) HCSNP; (e, f) High resolution energy spectra of N 1s and P 2p of HCSNP.

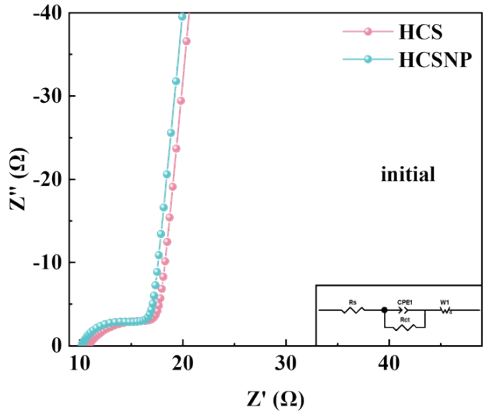

Fig. S9. EIS spectra and fitting circuits of HCS and HCSNP electrodes.

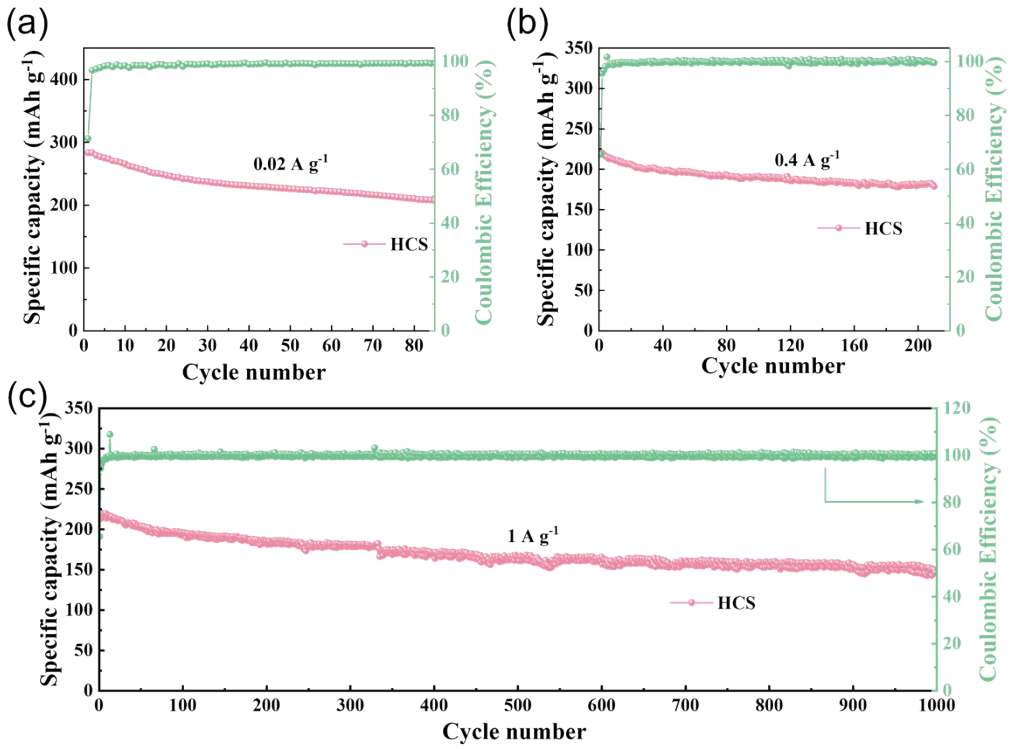

Fig. S10. Cycling performance of the HCS electrode: (a) at 0.02 A g^{-1}; (b) at 0.4 A g^{-1}; (c) at 1 A g^{-1}.

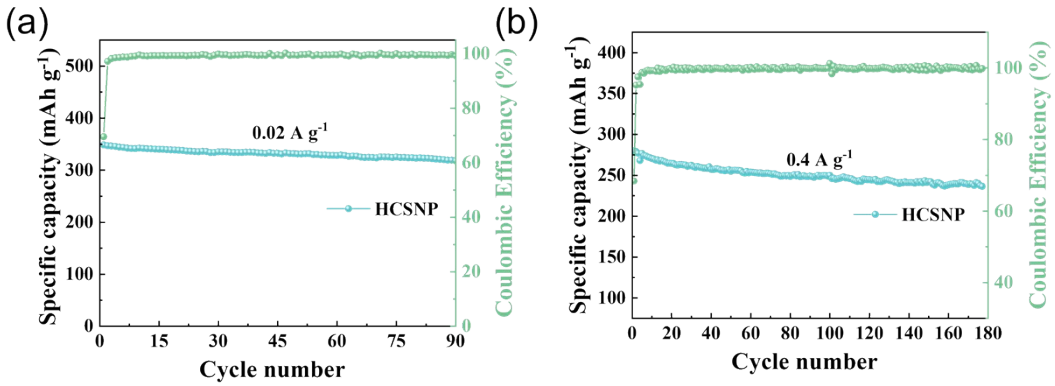

Fig. S11. Cycling performance of the HCSNP electrode: (a) at 0.02 A g^{-1}; (b) at 0.4 A g^{-1}.

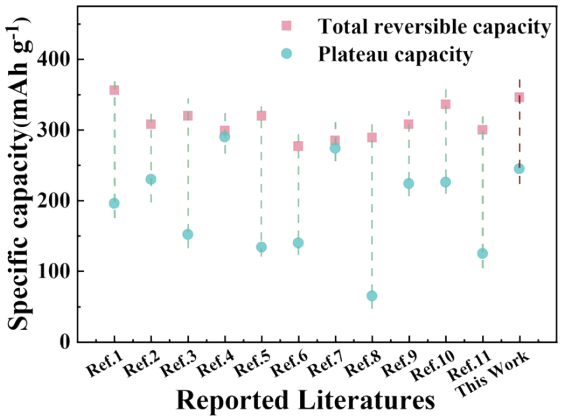

Fig. S12. Comparison diagram of the reversible specific capacity/plateau capacity of the HCSNP electrode with recently reported hard carbon anodes [1-11].

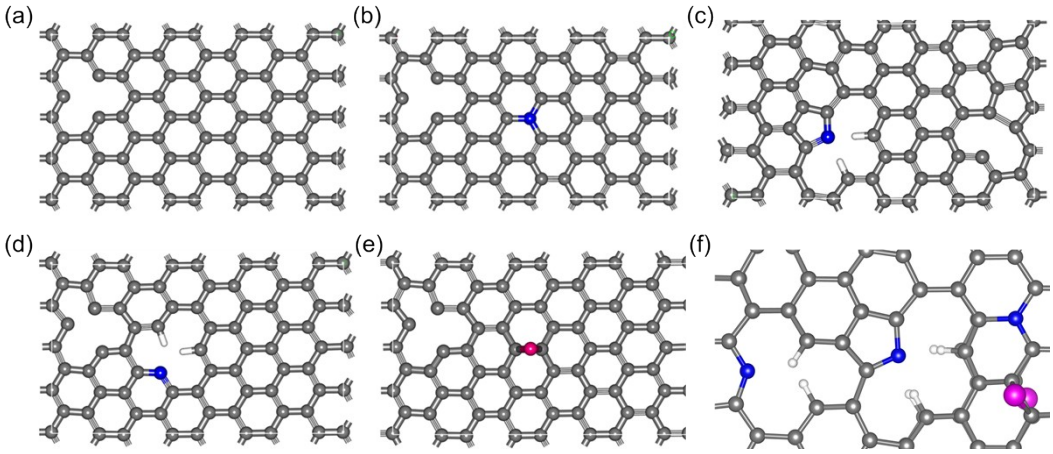

Fig. S13. Theoretical models: (a) PGs; (b) Q-NDGs; (c) Pyrr-NDGs; (d) Pyri-NDGs; (e) PDGs; (f) N/P-DGs.

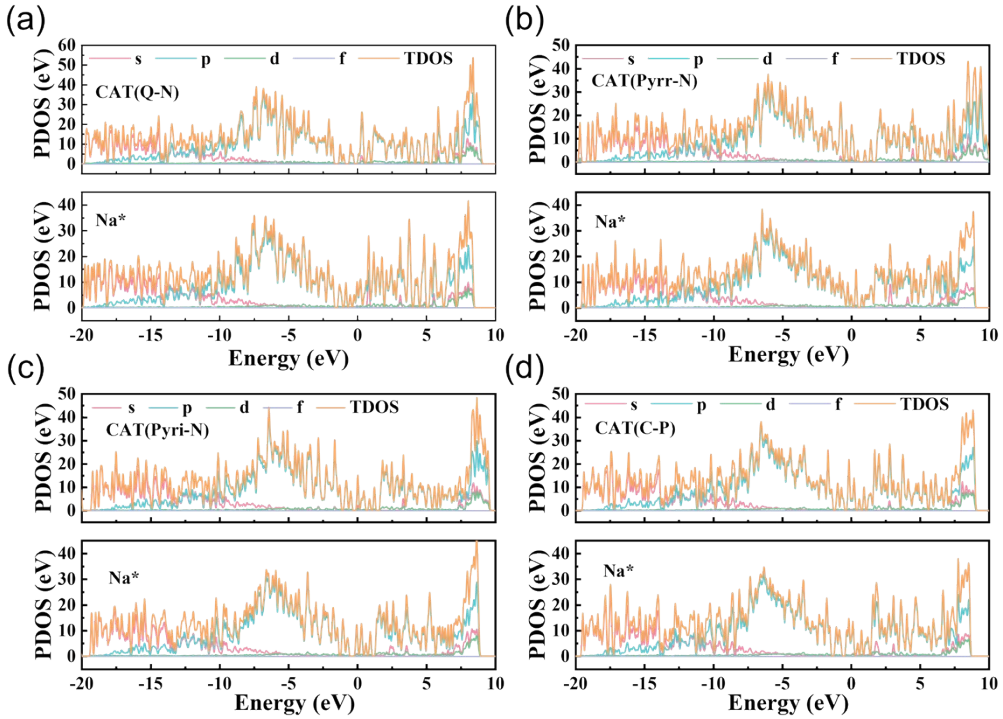

Fig. S14. The changes in the density of states of Na before and after adsorption in Q-NDGs, Pyrr-NDGs, Pyri-NDGs, and PDGs.

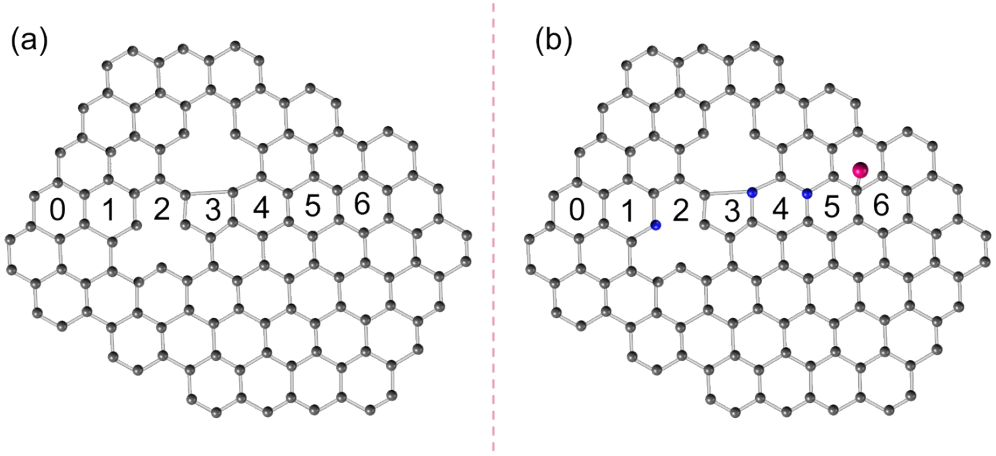

Fig. S15. Schematic diagrams of the diffusion position of Na in PGs and N/P-DGs.

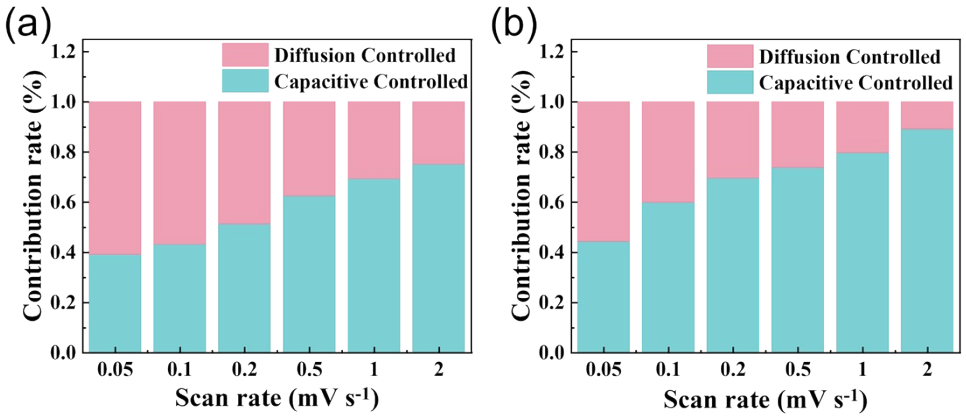

Fig. S16. The proportion of diffusion-controlled behavior and capacitive controlled behavior at different scan rates: (a) HCS electrode and (b) HCSNP electrode.

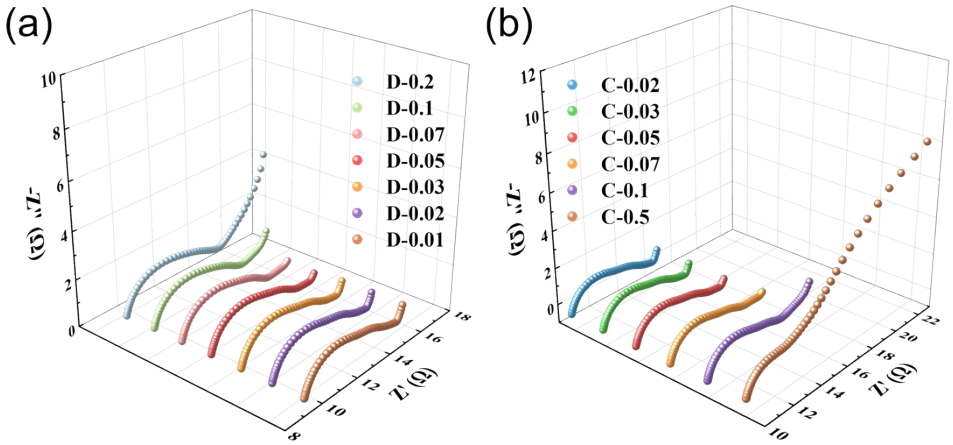

Fig. S17. In-situ EIS spectra of the HCS electrode: (a) the discharging process and (b) the charging process.

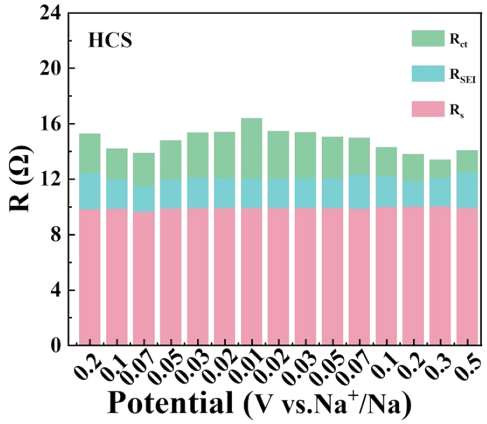

Fig. S18. Fitted impedance values of the HCS electrode.

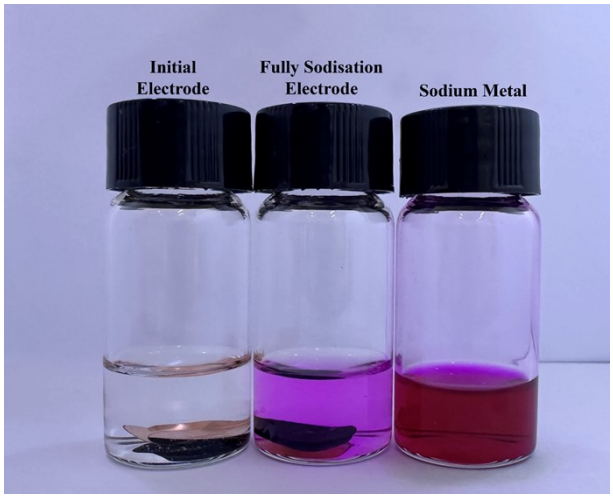

Fig. S19. Color changes of the reference samples reacting with a 1% phenolphthalein ethanol solution: The samples from left to right are the original HCSNP electrode, the fully discharged HCSNP electrode, and metallic sodium.

2 Tables

Table 1 Fitting of R_s, R_{SEI}, R_{ct} and W based on the equivalent circuit.

Table 1 (a) Fitting information of the initial HCS and HCSNP electrodes.

Initial	HCS	HCSNP
R_s (Ω)	10.79	10.05
R_{ct} (Ω)	4.458	3.484
W (Ω)	10.11	7.29

Table 1 (b) Fitting information of the HCS and HCSNP electrodes after one cycle.

After the 1st cycle	HCS	HCSNP
R_s (Ω)	8.207	9.147
R_{SEI} (Ω)	5.455	14.887
R_{ct} (Ω)	6.186	87.121
W (Ω)	911.7	763.7

Table 1 (c) Fitting information of the HCS and HCSNP electrodes after ten cycles.

After the 10th cycle	HCS	HCSNP
R_s (Ω)	8.205	9.1243
R_{SEI} (Ω)	4.13	11.12
R_{ct} (Ω)	5.809	15.27
W (Ω)	926.2	897.3

References

[1] H. Chen, N. Sun, Q.-Z. Zhu, R.-A. Soomro, B. Xu, Adv. Sci. 9 (2022) 2200023.

[2] Y.-F. Chen, H.-Y. Sun, X.-X. He, Q.-H. Chen, J.-H. Zhao, Y.-H. Wei, X.-Q. Wu, Z.-J. Zhang, Y. Jiang, S.-L. Chou, Small. 20 (2024) 2307132.

[3] H.-N. He, J. He, H.-B. Yu, L. Zeng, D. Luo, C.-H. Zhang, Adv. Energy Mater. 13 (2023) 2300357.

[4] X.-X. He, W.-H. Lai, Y. Liang, J.-H. Zhao, Z. Yang, J. Peng, X.-H. Liu, Y.-X. Wang, Y. Qiao, L. Li, X.-Q. Wu, S.-L. Chou, Adv. Mater. 35 (2023) 2302613.

[5] Y.-J. Huang, X. Zhong, X.-Y. Hu, Y. J. Li, K. Wang, H.-Y. Tu, W.-T. Deng, G.-Q. Zou, H.-S. Hou, X.-B. Ji, Adv. Funct. Mater. 34 (2024) 2308392.

[6] L.-C. Ji, Y. Zhao, L.-J. Cao, Y. Li, C.-L. Ma, X.-G. Qi, Z.-P. Shao, J. Mater. Chem. A. 11 (2023) 26727-26741.

[7] G.-W. Lee, K. Bin MIN, M.-E. Lee, Y.-K. Lee, H.-R. Lee, S.-S. Kim, S.-Y. Cho, H.-I. Joh, Y.-K. Kim, S.-H. Lee, Chem. Eng. J. 479 (2024) 147766.

[8] Y. Liu, Y.-H. Wan, J.-Y. Zhang, X.-M. Zhang, C.-T. Hung, Z.-R. Lv, W.-M. Hua, Y.-G. Wang, D.-L. Chao, W. Li, Small, 19 (2023) 2301203.

[9] K.-F. Wang, F. Sun, H. Wang, D.-Y. Wu, Y.-X. Chao, J.-H. Gao, G.-B. Zhao, Adv. Funct. Mater. 32 (2022) 2203725.

[10] J.-H. Zhao, X.-X. He, W.-H. Lai, Z. Yang, X.-H. Liu, L. Li, Y. Qiao, Y. Xiao, L. Li, X.-Q. Wu, S.-L. Chou, Adv. Energy Mater. 13 (2023) 2300444.

[11] Y.-H. Zhao, Z. Hu, C.-L. Fan, P. Gao, R.-S. Zhang, Z.-X. Liu, J.-S. Liu, J.-L. Liu, Small, 19 (2023) 2303296.